Asynchronous stoichiometric response in lithium iron phosphate batteries

William A. Paxton,[a] E. Koray Akdoğan, İlyas Şavkliyildiz, Ankur U. Choksi, Scott X. Silver, and Thomas Tsakalakos
Materials Science and Engineering, Rutgers, The State University of New Jersey, Piscataway, New Jersey 08854, USA

Zhong Zhong
Photon Sciences, Brookhaven National Laboratory, Upton, New York 11973, USA

(Received 15 June 2014; accepted 8 October 2014)

Operando energy-dispersive x-ray diffraction (EDXRD) was carried out on a newly formed 8 Ah lithium iron phosphate ($LiFePO_4$) battery with the goal of elucidating the origin of asynchronous phase transformation commonly seen with in situ x-ray diffraction studies. The high-energy photons at the NSLS X17B1 beamline allow for penetration into a fully assembled battery and therefore negate any need for a specially designed in situ cell which often uses modified current collectors to minimize x-ray attenuation. Spatially-and-temporally resolved phase-mapping was conducted with a semiquantitative reference intensity ratio (RIR) analysis to estimate the relative abundance of the delithiated phase. The data show an asynchronous response in the stoichiometry versus the electrochemical profile and suggest limited diffusion in the electrode toward the end of discharge. Our results confirm that the asynchronous electrode response is not just limited to specially designed cells but occurs in fully assembled cells alike. We attribute this behavior to be a consequence of performing a local measurement over a wide-area heterogeneous reaction.

I. INTRODUCTION

The use of lithium-ion batteries in portable electronics has enabled a proliferation of devices in recent years. Still, the present-and-future requirements of energy storage for transportation and grid applications are not yet met by available technologies. Specifically, energy density, power capability, cycle life, calendar life, and safety all need improvement. Low-cost manufacturing will also be required for lithium-ion batteries to compete with existing power infrastructure.[1–3]

One of the main hindrances in the progress of battery research is that the constituent electrode materials are inaccessible once an electrochemical cell is constructed. This leaves the researcher with a limited number of available feedback mechanisms to assess the cell's performance, e.g., current, voltage, and impedance. Indeed, there is a whole scientific community dedicated to the study and modeling of such electrochemical data.[4] However, these data are limited in their ability to reveal the more-localized smaller-scale structural mechanisms on which the batteries' performance is so dependent.[5]

In the last 20 years great advancement has been made in the area of in situ characterization using x-rays, enabling researchers to study battery materials without removing them from a cell. Aside from improvements in probe brightness and detector efficiency, these advancements can largely be credited to the construction of new cell designs utilizing low-absorption encapsulation and current-collector materials, thus allowing for greater penetration of x-rays. Such work has enabled discovery of hidden phases and the screening of potential future electrode materials.[6–9]

Of those materials, olivine structured lithium iron phosphate, $LiFePO_4$, shows great promise as an electrode, due to its superior thermal stability, relatively low cost, and high capacity retention during cycling.[10–13] Despite intrinsically low electronic and ionic conductivity, its use in commercial batteries has become a reality through the engineering of particle morphology and composition.[10–13] Still, the exact nature of the phase transformation during lithiation is elusive, despite many theoretical and in situ studies.[14]

It is understood that the phase transformation upon lithiation of $FePO_4$ is first order which gives way to a characteristic flat voltage response and biphasic composition with very limited solid solution regions at the end-member phases.[10–14] This has been confirmed by a multitude of in situ studies of the lithiation and delithiation processes in which researchers have compared structural measurements to the electrochemical response.[15–17] Disregarding the limited solid-solution ranges, one can consider the equation $FePO_4 + Li^+ + e^- \rightleftarrows LiFePO_4$. This

[a]Address all correspondence to this author.
e-mail: will.paxton@rutgers.edu
DOI: 10.1557/jmr.2014.321

 © Materials Research Society 2014

https://doi.org/10.1557/jmr.2014.321 Published online by Cambridge University Press

shows that for each lithium ion that intercalates, an electron is generated and the lithiated phase is created. However, in some cases anomalous behavior has been observed; that is to say that after extracting X% of the electrons from the system, the phase fraction observed deviates far from X%.[18–23] There are quite a few explanations of this so-called asynchronous phase transition behavior, ranging from effects of polaron formation in the lattice[14] to the existence of a nonrepresentative x-ray volume measured in a heterogeneous electrode.[23,24] While both are possible, the most recent modeling efforts[25] and the work of others[16] suggest that heterogeneous microstructure and electrical conductivity of the electrode play a large role in the phase transformation behavior.

Energy-dispersive x-ray diffraction (EDXRD) is well established as a viable tool for in situ battery characterization.[26–30] Additionally, recent studies utilizing synchrotron radiation have shown very powerful spatial-and-temporal mapping capabilities.[28–30] The ultrahigh energy x-rays available (up to 200 keV) from the X17 superconducting-wiggler beamport at the National Synchrotron Light Source give way to low absorption losses and enable operando measurements.[28–30] Here, we use the term operando to differentiate the ability of EDXRD to take measurements in fully assembled cells without special sample preparation. In this study we use the unique operando spatial and temporal mapping capabilities of EDXRD to study the response of a lithium iron phosphate electrode in an actual production battery. We intend to elucidate any spatial effects which may contribute to the asynchronous phase transition behavior.

II. EXPERIMENTAL

The lithium-ion battery that was chosen for this operando study was a fully assembled 10 Ah lithium iron phosphate polymer cell. To achieve a capacity of 10 Ah, the internal structure of the cell consisted of multiple repeating units of electrodes, current collectors, and separator materials in a prismatic layout. The positive electrodes were comprised of nanosized lithium iron phosphate which were coated in carbon for increased electrical conductivity. The negative electrode consisted of graphitic carbon. The cell was recently assembled with no prior history, besides formation cycles, and was therefore considered new.

X-ray diffraction measurements were conducted at the superconducting wiggler beamline X17B1 of The National Synchrotron Light Source at Brookhaven National Laboratory. The superconducting wiggler provides a spectral flux with high brilliance across a wide range of energies up to 200 keV.[31] In an EDXRD measurement the Bragg condition for diffraction is satisfied by the use of polychromatic radiation, therefore allowing measurements at a fixed angle. Experiments were carried out in Laue geometry which results in a fixed diffraction volume in space, commonly referred to as the gage volume (GV), with a parallelepiped geometry. Figure 1 gives a schematic of the configuration.

The governing equation for EDXRD is given by

$$E_{hkl} = \frac{6.199}{\sin\theta\, d_{hkl}} \quad ,$$

where E is the energy in keV and d_{hkl} is the interatomic spacing associated with the plane hkl measured in Angstroms. The photons are collected and their energy is measured using a germanium detector. The photon counts are then binned into 8192 channels using a multichannel analyzer. The energy calibration is done later by the use of LaB_6 and CeO_2 standards.

A Bragg angle of $2\theta = 3°$ was used and the slits were arranged such that a GV with dimensions of approximately 3 mm × 3 mm × 30 μm is formed. The 30 μm height of the GV gives rise to a thickness that is commensurate with that of the individual electrode layer in the cell. This is important for phase-mapping ability because one is able to obtain a distinct signal from one electrode layer rather than multiple layers. The battery was carefully placed and leveled on a sample holder that can move in x, y, and z directions with accuracy of 0.1 μm.

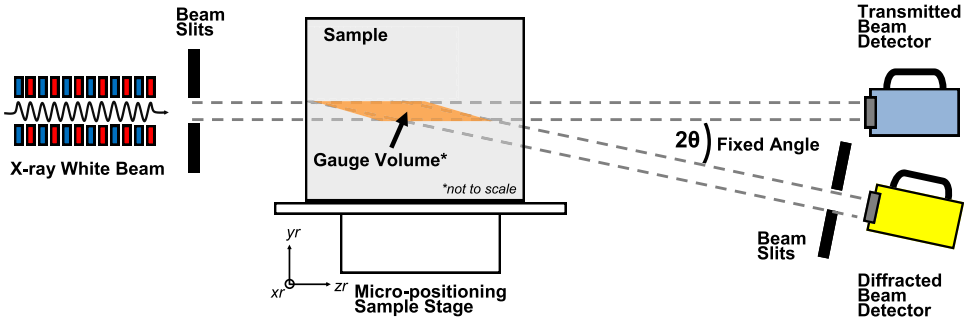


FIG. 1. Schematic depicting the experimental configuration of the X17B1 beamline at NSLS. The high energy polychromatic x-rays are collimated through a series of slits and imposed on a sample which can move in all three dimensions. Within the GV, the material scatters the x-rays where they are collected by an energy detector at a fixed angle.

https://doi.org/10.1557/jmr.2014.321 Published online by Cambridge University Press

The orientation of the cell placement with respect to the beam is shown in Fig. 2(a). A very accurate tomographic profile of the cell was obtained and served as a map of the internal structure of the cell. This is achieved by scanning the GV through the entire thickness of the cell and then plotting the total scattered intensity as a function of position. Such a plot was used to calibrate the experiment and locate an area of interest. The tomographic profile is shown, along with the area of interest, in Fig. 2(b). With the cell fully charged, a sequence of 15 diffraction spectra were collected as a function of depth in the yr-direction. The area of study was in the body-center of the cell and the collection time for each spectrum was 45 s. Using a battery cycler (Arbin BT2000, Arbin Instruments, College Station, TX), the cell was then discharged at a constant current of 2 amperes which corresponds to a C-rate of C/5. Every 45 min, the discharge procedure was halted and, after a relaxation time

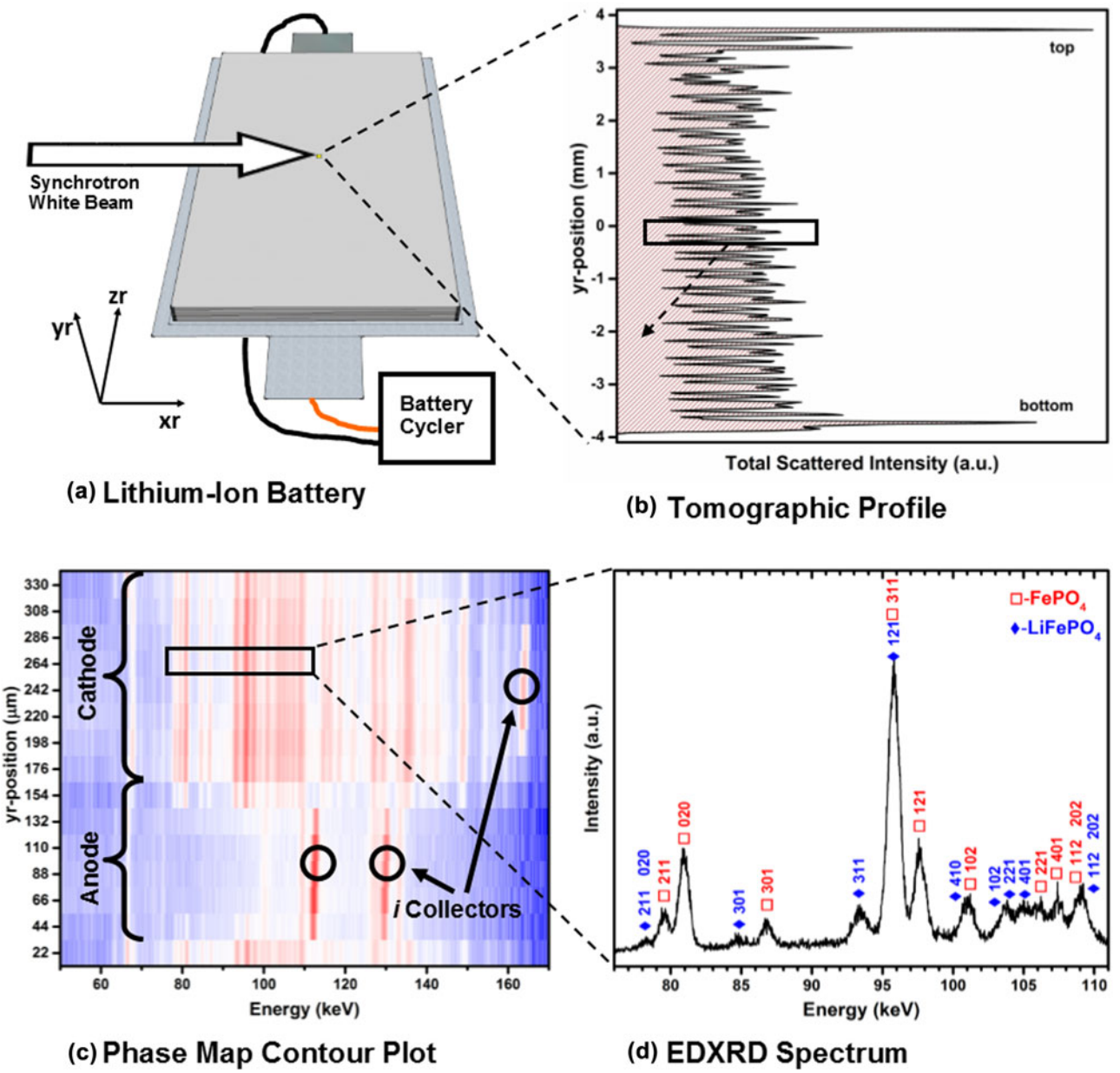


FIG. 2. Summary of the characterization capabilities of EDXRD as they relate to lithium-ion batteries. (a) Depiction of the lithium-ion battery in relation to the synchrotron beam along with the experimental coordinates. The cell is also connected to a battery cycler. (b) A tomographic profile of the internal structure of the cell is shown by plotting the total scattered intensity as a function of position. The plot is rotated to remain consistent with the experimental coordinates. (c) A contour plot of the scans across a selected region inside the cell is given for the purpose of phase mapping. The electrodes of the cell are identified as well as the current collectors. (d) A single EDXRD spectrum of an area within the cathode region. The Bragg reflections of two phases are labeled.

https://doi.org/10.1557/jmr.2014.321 Published online by Cambridge University Press

of 5 min, depth profiles were taken. This procedure was repeated throughout the discharge cycle for a total collection of nine depth profiles.

The relative amounts of $FePO_4$ and $LiFePO_4$ phases were determined semiquantitatively using a Gaussian peak-fitting routine found in the software, Fityk.[32] The $FePO_4$ (020) and the $LiFePO_4$ (311) reflections were chosen because they had the best combination of intensity and isolation from any other reflection. However, surrounding reflections were also fit to isolate their contributions. Additionally, since the GV is much larger than the crystallites measured, we assume there to be no texture related effects and a single reflection to be a good representation of the phase as a whole. The integrated intensities (area under the curve) of each peak were used to compute the weight fractions of each phase using the reference intensity ratio (RIR) method.[33] In this analysis, the ratio of the intensities is weighted using their reference values (I_{rel}) and their ratio to a known standard of corundum (RIR_c) shown in the following equation. The I_{rel} and RIR_c values used for the analysis were 62.72 and 1.49 for $FePO_4$,[34] and 92.75 and 1.32 for $LiFePO_4$ (Ref. 35), respectively. The mole fraction can then be calculated by dividing the weight fraction by the molar mass. Furthermore, showing the mole fraction of the $FePO_4$ phase can be a convenient indicator of the remaining capacity in the volume measured, thereby leading to a spatially resolved phase mapping.[24] It is also important to note, since the analysis compares two phases within each spectrum, it negates any need to consider current-decay effects from the synchrotron ring when comparing different locations and time-points as long as the signal strength is sufficiently above the experimental noise as it was throughout the experiments.

After the synchrotron experiment, the fully discharged cell was disassembled in an argon-filled glove box. The approximate area of interest was cut away and mounted to a sample-stud using carbon tape. Images were taken for analysis using a field-emission scanning electron microscope (Zeiss).

III. RESULTS AND DISCUSSION

A summary of the measurements collected from the battery is shown in Fig. 2. As previously mentioned, Fig. 2(a) shows the orientation of the cell with the beam, and Fig. 2(b) shows the tomographic profile of internal layered structure. Figure 2(c) shows a diffraction contour plot with energy on the *x*-axis and position on the *y*-axis. In this plot, the cathode and anode regions of the cell are indicated as the characteristic Bragg lines of the current collectors. The cathode region is identified as a two-phase mixture of $FePO_4$ and $LiFePO_4$. Also in the cathode region is an aluminum current collector. The anode region can be seen with much fewer lines; identified as lithiated graphite and a copper current collector. We assume there to be some curvature of the electrode layers which would explain the small juxtaposition of the current collector and electrode phases. Figure 2(d) shows selected diffraction spectra from the contour map with the Bragg peaks of both lithiated and nonlithiated phases identified.

The cell potential curve during discharge is shown in Fig. 3. The numbers indicate the points at which the discharge was halted and diffraction spectra were collected. The cell provided a flat voltage profile which is indicative of the first-order phase transformation. Small drops in the voltage can be seen when the discharge starts after each scan which is caused by the internal resistance of the cell. The overall capacity of the cell is what we expected.

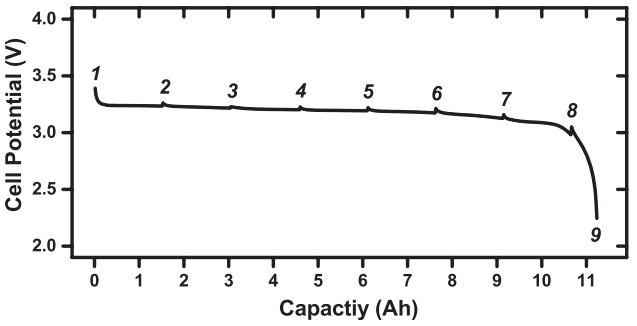


FIG. 3. The cell potential as a function of capacity obtained when discharging the cell. The times at which the discharge was stopped and diffraction spectra collected are indicated by the numbers above the curve.

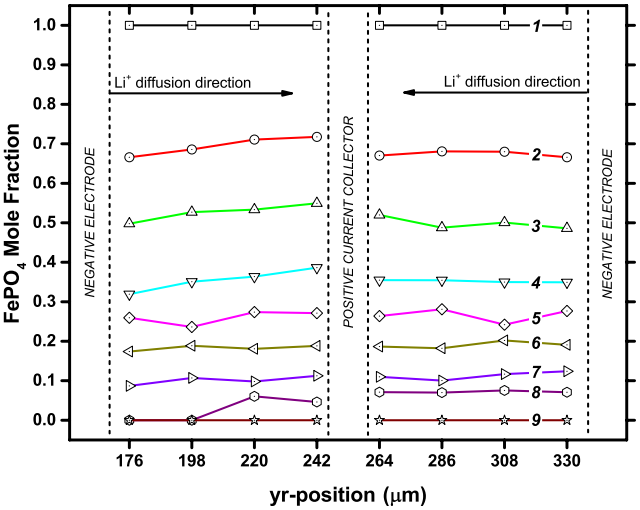


FIG. 4. Time evolution of the iron phosphate mole fraction as a function of position (depth) in the electrode layer. As the cell is discharged, the iron phosphate phase is converted to lithium iron phosphate by the diffusion of lithium ions into the positive electrode from the negative electrode. The numbers of the lines indicate the time depicted in Fig. 3.

https://doi.org/10.1557/jmr.2014.321 Published online by Cambridge University Press

A more detailed phase mapping of the positive electrode is shown in Fig. 4. Here we show the space-time evolution of the electrode with the $FePO_4$ mole fraction as a function of depth in the electrode. As the cell is discharged, the iron phosphate phase is converted to lithium iron phosphate by the diffusion of lithium ions into the cathode from the electrolyte, with an accommodating change of valence state of the Fe in the lattice. The variation of composition as a function of depth appears to be relatively linear in most scans. The only pronounced area where it is not is in scan number 8 where the edge closest to the separator and anode (lithium source) is fully lithiated. This shows evidence of lower diffusion mobility toward the later part of the discharge. Based on these data, it is not possible to say what exactly is limiting diffusion, but the fact that the diffusion mobility is only observed toward the end of the battery's discharge cycle, coinciding with where there is a larger deviation from equilibrium voltage, suggests that the two may be correlated. This is consistent with the model used by Farkhondeh et al. for bulk behavior dominated by heterogeneous conductive coatings on a poor electronic conductor.[25]

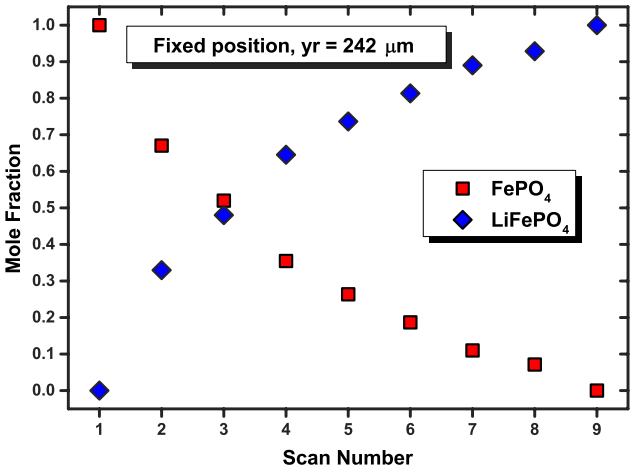


FIG. 5. Mole fraction of $FePO_4$ and $LiFePO_4$ phases at the position which is centrally located in the electrode. The measured fractions of each phase show the asynchronous electrode utilization behavior.

The data in Fig. 4 also show a deviation from ideal-stoichiometric behavior in the electrode, similar to that of the previously hypothesized asynchronous phase transformation. Since the cell was discharged at a constant current and the diffraction spectra were taken at equal intervals, we expected to see a linear response in the transformation of $FePO_4$ to $LiFePO_4$; a 1:1 relationship

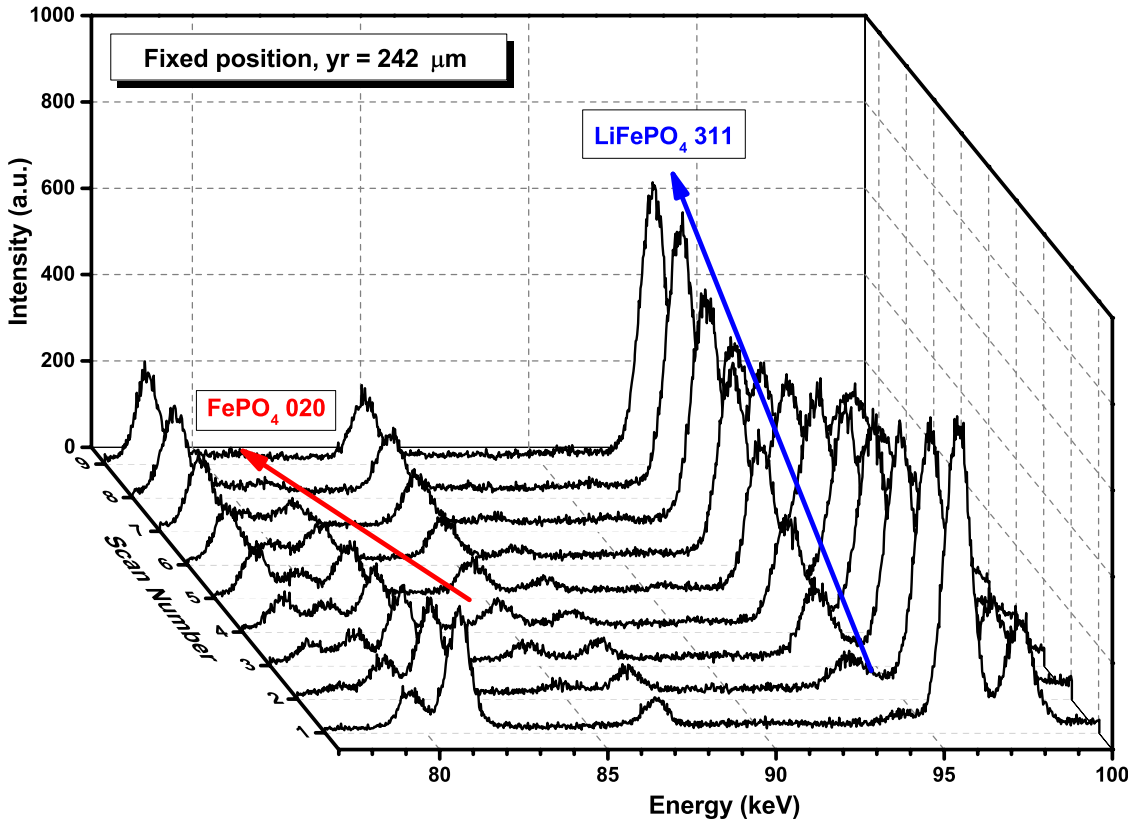


FIG. 6. Waterfall plot of the 9 spectra collected in a fixed position at 242 μm, which is approximately the center of the electrode depth. The $FePO_4$ (020) and $LiFePO_4$ (311) peaks are labeled, indicating the reflections used for the mole fraction analysis.

https://doi.org/10.1557/jmr.2014.321 Published online by Cambridge University Press

of Li^+ to e^-. However, after the first discharge interval, the amount of $FePO_4$ converted to $LiFePO_4$ was approximately 30%. This number appears to decrease as the battery is discharged further. Additionally, the time and space mapping shows that the observed asynchronous electrode utilization phenomenon appears consistent throughout the depth of the electrode. Since the effect is consistent throughout the electrode, we decided to plot just the evolution of both phases in the region in electrodes center. This is shown in Fig. 5 where the asynchronous response can be seen more clearly. A waterfall plot of the nine diffraction spectra used for the RIR analysis is shown in Fig. 6. The peaks used for analysis, $FePO_4$ 020 at ~81 keV and $LiFePO_4$ 311 at ~93 keV, are labeled and show suitable intensity for the analysis.

Figure 7 shows a field-emission scanning electron micrograph of the positive electrode from the disassembled sample. The iron phosphate cathode powder appears to have nanosized grains but also larger grains and agglomerations. Additionally, the particles appear to be quite heterogeneous with a fairly broad size distribution and varying morphologies. Evidence of fracturing also suggests the presence of electrochemical-induced strains which can occur from the volume changes associated with lithium intercalation. We postulate that the material heterogeneity contributes to a spatially heterogeneous reaction-front within the electrode, thus influencing a localized asynchronous response.

While we observe the asynchronous electrode response, the origins of which still remain elusive. We postulate that the asynchronous response is a localization phenomenon, the result of variances in the electrode/electrolyte/current-collector interfaces and/or the surface treatments of the particles. This is certainly possible considering the measurements presented in this study represent less than 1% of the total contributing electrode. Powder heterogeneity observed by electron microscopy further corroborate a localization phenomenon. However, additional experiments are required to fully determine the origin of asynchronous behavior. Further experiments where we investigate different areas of the cell are under way. If we observe the asynchronous response in one area and a complementary behavior in another, we may be able to confirm that it is a localization phenomenon caused by heterogeneous microstructure and conductive contact, provided that the areas average out to a more linear electrode response.

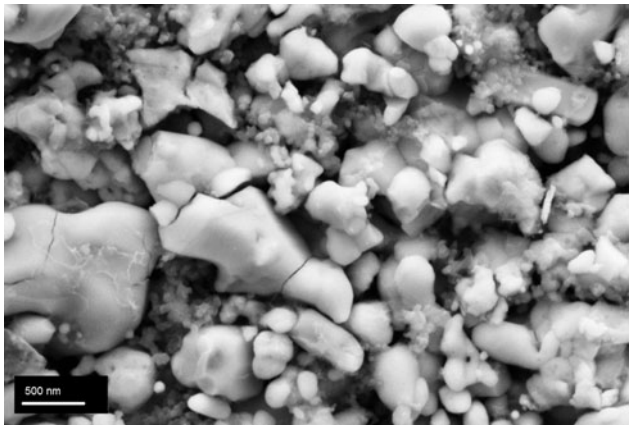


FIG. 7. Scanning electron micrograph of the positive electrode. The sample was obtained by disassembling the fully discharged cell under a glove box and cutting away the area of the cell that was measured. The image shows a heterogeneous powder with fractured grains and a broad size distribution.

IV. CONCLUDING REMARKS

We have conducted operando EDXRD measurements on a full-sized lithium iron phosphate battery and a succinct overview of the measurement capabilities is given. Spatially and temporally resolved phase mapping was achieved at nine different time points while discharging the battery. A mole fraction phase analysis using the RIR method was completed for the positive electrode. The results show limited diffusion toward the end of the discharge cycle as well as an asynchronous electrode utilization response. The results confirm that the asynchronous behavior is not just an artifact of in situ cell designs but occurs in fully assembled batteries as well. We attribute this behavior to be a consequence of performing a local measurement over a wide-area heterogeneous reaction.

ACKNOWLEDGEMENTS

Use of the National Synchrotron Light Source, Brookhaven National Laboratory, was supported by the U.S. Department of Energy, Office of Science, Office of Basic Energy Sciences, under Contract No. DE-AC02-98CH10886.

REFERENCES

1. M. Armand and J.M. Tarascon: Building better batteries. *Nature* **451**, 652–657 (2008).
2. B. Scrosati and J. Garche: Lithium batteries: Status, prospects and future. *J. Power Sources* **195**, 2419–2430 (2009).
3. J.R. Croy, A. Abouimrane, and Z. Zhang: Next-generation lithium-ion batteries: The promise of near-term advancements. *MRS Bull.* **39**(5), 407 (2014).
4. T.B. Reddy: *Linden's Handbook of Batteries*, 4th ed. (McGraw-Hill, New York, 2011).
5. M. Ebner, F. Marone, M. Stampanoni, and V. Wood: Visualization and quantification of electrochemical and mechanical degradation in Li ion batteries. *Science* **342**(6159), 716–720 (2013).
6. J.N. Reimers and J.R. Dahn: Electrochemical and in situ x-ray diffraction studies of lithium intercalation in Li_xCoO_2. *J. Electrochem. Soc.* **139**(8), 2091–2097 (1992).
7. G.G. Amatucci, J.M. Tarascon, and L.C. Klein: CoO_2, the end member of the Li_xCoO_2 solid solution. *J. Electrochem. Soc.* **143**(3), 1114–1123 (1996).

https://doi.org/10.1557/jmr.2014.321 Published online by Cambridge University Press

8. M. Morcrette, Y. Chabre, G. Vaughan, G. Amatucci, J-B. Leriche, S. Patoux, C. Masquelier, and J-M. Tarascon: In situ x-ray diffraction techniques as a powerful tool to study battery electrode materials. *Electrochim. Acta* **47**(19), 3137–3149 (2002).
9. M.A. Rodriguez, D. Ingersolla, S.C. Vogel, and D.J. Williams: Simultaneous in situ neutron diffraction studies of the anode and cathode in a lithium-ion cell. *Electrochem. Solid-State Lett.* **7**(1), A8–A10 (2004).
10. A.K. Padhi, K.S. Nanjundaswamy, and J.B.D. Goodenough. Phospho-olivines as positive-electrode materials for rechargeable lithium batteries. *J. Electrochem. Soc.* **144**, 1188–1194 (1997).
11. A. Yamada, S.C. Chung, and K. Hinokuma: Optimized $LiFePO_4$ for lithium battery cathodes. *J. Electrochem. Soc.* **148**, A224 (2001).
12. S-Y. Chung, J.T. Bloking, and Y-M. Chiang: Electronically conductive phospho-olivines as lithium storage electrodes. *Nat. Mater.* **1**(2), 123–128 (2002).
13. W-J. Zhang: Structure and performance of $LiFePO_4$ cathode materials: A review. *J. Power Sources* **196**(6), 2962–2970 (2011).
14. Corey T. Love, Anna Korovina, Christopher J. Patridge, Karen E. Swider-Lyons, Mark E. Twigg, and David E. Ramaker: Review of $LiFePO_4$ phase transition mechanisms and new observations from x-ray absorption spectroscopy. *J. Electrochem. Soc.* **160**(5), A3153–A3161 (2013).
15. A.S. Andersson, B. Kalska, L. Haggstrom, and J.O. Thomas: Lithium extraction/insertion in $LiFePO_4$: An x-ray diffraction and Mössbauer spectroscopy study. *Solid State Ionics* **130**, 41–52 (2000).
16. C. Delmas, M. Maccario, L. Croguennec, F. Le Cras, and F. Weill: Lithium deintercalation in $LiFePO_4$ nanoparticles via a domino-cascade model. *Nat. Mater.* **7**, 665–671 (2008).
17. N. Meethong, Y-H. Kao, M. Tang, H-Y. Huang, W.C. Carter, and Y-M. Chiang: Electrochemically induced phase transformation in nanoscale olivines $Li_{1-x}MPO_4$ (M = Fe, Mn). *Chem. Mater.* **20**, 6189–6198 (2008).
18. H-H. Chang, C-C. Chang, H-C. Wu, M-H. Yang, H-S. Sheu, and N-L. Wu: Study on dynamics of structural transformation during charge/discharge of $LiFePO_4$ cathode. *Electrochem. Commun.* **10**(2), 335–339 (2008).
19. H.C. Shin, K.Y. Chung, W.S. Min, D.J. Byun, H. Jang, and B.-W. Cho: Asymmetry between charge and discharge during high rate cycling in $LiFePO_4$ – In situ x-ray diffraction study. *Electrochem. Commun.* **10**(4), 536–540 (2008).
20. K. Inoue, S. Fujieda, K. Shinoda, S. Suzuki, and Y. Waseda: Chemical state of iron of $LiFePO_4$ during charge-discharge cycles studied by in-situ x-ray absorption spectroscopy. *Mater. Trans.* **51**(12), 2220–2224 (2010).
21. J.B. Leriche, S. Hamelet, J. Shu, M. Morcrette, C. Masquelier, G. Ouvrard, M. Zerrouki, P. Soudan, S. Belic, E. Elkaïm, and F. Baudelet: An electrochemical cell for operando study of lithium batteries using synchrotron radiation. *J. Electrochem. Soc.* **157**(5), A606–A610 (2010).
22. H.C. Shin, K.W. Nam, Y.W. Chang, B.W. Cho, W-S. Yoon, X-Q. Yang, and K.Y. Chung: Comparative studies on C-coated and uncoated $LiFePO_4$ cycling at various rates and temperatures using synchrotron based in situ x-ray diffraction. *Electrochim. Acta* **56**(3), 1182–1189 (2011).
23. X-J. Wang, C. Jaye, K-W. Nam, B. Zhang, H-Y. Chen, J. Bai, H. Li, X. Huang, D.A. Fischer, and X-Q. Yang: Investigation of the structural changes in $Li_{1-x}FePO_4$ upon charging by synchrotron radiation techniques. *J. Mater. Chem.* **21**, 11406–11411 (2011).
24. J. Liu, M. Kunz, K. Chen, N. Tamura, and T.J. Richardson: Visualization of charge distribution in a lithium battery electrode. *J. Phys. Chem. Lett.* **1**(14), 2120–2123 (2010).
25. M. Farkhondeh, M. Safari, M. Pritzker, M. Fowler, Taeyoung Han, Jasmine Wang, and C. Delacourt: Full-range simulation of a commercial $LiFePO_4$ electrode accounting for bulk and surface effects: A comparative analysis. *J. Electrochem. Soc.* **161**(3), A201–A212 (2014).
26. F. Ronci, B. Scrosati, V. Rossi Albertini, and P. Perfetti: A novel approach to in situ diffractometry of intercalation materials: The EDXD technique preliminary results on $LiNi_{0.8}Co_{0.2}O_2$. *Electrochem. Solid-State Lett.* **3**(4), 174–177 (2000).
27. S. Panero, P. Reale, F. Ronci, B. Scrosati, P. Perfetti, and V. Rossi Albertini: Refined, in-situ EDXD structural analysis of the $Li[Li_1/3Ti_5/3]O_4$ electrode under lithium insertion–extraction. *Phys. Chem. Chem. Phys.* **3**, 845–847 (2001).
28. J. Rijssenbeek, Y. Gao, Z. Zhong, M. Croft, N. Jisrawi, A. Ignatov, and T. Tsakalakos: In situ x-ray diffraction of prototype sodium metal halide cells: Time and space electrochemical profiling. *J. Power Sources* **196**(4), 2332–2339 (2011).
29. E. Takeuchi, A. Marschilok, K. Takeuchi, A. Ignatov, Z. Zhong, and M. Croft: Energy dispersive x-ray diffraction of lithium–silver vanadium phosphorous oxide cells: In situ cathode depth profiling of an electrochemical reduction–displacement reaction. *Energy Environ. Sci.* **6**, 1465–1470 (2013).
30. J.W. Gallaway, C.K. Erdonmez, Z. Zhong, M. Croft, L.A. Sviridov, T.Z. Sholklapper, D.E. Turney, S. Banerjee, and D.A. Steingart: Real-time materials evolution visualized within intact cycling alkaline batteries. *J. Mater. Chem. A* **2**, 2757–2764 (2014).
31. W. Thomlinson, D. Chapman, N. Gmür, and N. Lazarz: The superconducting wiggler beamport at the National Synchrotron Light Source. *Nucl. Instrum. Methods A* **266**, 226–233 (1988).
32. M. Wojdyr: Fityk: A general-purpose peak fitting program. *J. Appl. Crystallogr.* **43**, 1126–1128 (2010).
33. F.H. Chung: Quantitative interpretation of x-ray diffraction patterns of mixtures. III. Simultaneous determination of a set of reference intensities. *J. Appl. Crystallogr.* **8**, 17 (1975).
34. Calculated from FIZ#99861 (09/11/09) by Jade for FePO.
35. Calculated from FIZ#162282 (09/11/09) by Jade for LiFePO.

Supplementary Material

To view the supplementary material for this article, please visit http://dx.doi.org/jmr.2014.321.

https://doi.org/10.1557/jmr.2014.321 Published online by Cambridge University Press